Talanta 275 (2024) 126095

Contents lists available at ScienceDirect

Talanta

journal homepage: www.elsevier.com/locate/talanta

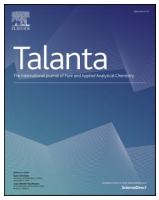

Controlled silver electrodeposition on gold nanoparticle antibody tags for ultrasensitive prostate specific antigen sensing using electrochemical and optical smartphone detection

Guillermo Redondo-Fernández, Laura Cid-Barrio, María T. Fernández-Argüelles, Alfredo de la Escosura-Muñiz **, Ana Soldado *, José M. Costa-Fernández

Department of Physical and Analytical Chemistry, University of Oviedo, Avda. Julián Clavería 8, 33006, Oviedo, Spain

ARTICLE INFO

Handling editor: Agata Michalska

Keywords:
Immunosensor
Biomarker
Nanoparticle size-enhancement
Smartphone detection
Prostate specific antigen

ABSTRACT

One of the current challenges in medicine is to achieve a rapid and unequivocal detection and quantification of extremely low levels of disease biomarkers in complex biological samples. Here, we present the development and analytical evaluation of a low-cost smartphone-based system designed for ultrasensitive detection of the prostate-specific antigen (PSA) using two detection alternatives: electrochemical or optical, by coupling the smartphone with a portable potentiostat or magnifying lenses. An antibody tagged with gold nanoparticles (AuNPs), and indium tin oxide coated polyethylene terephthalate platform (ITO-PET) have been used to develop a sandwich-type immunoassay. Then, a controlled silver electrodeposition on the AuNPs surface is carried out, enhancing their size greatly. Due to such strong nanoparticle-size amplification (from nm to μm), the final detection can be dual, by measuring current intensity or the number of silver-enlarged microstructures generated. The proposed strategies exhibited limit detections (LOD) of 102 and 37 fg/mL for electrochemical and optical detection respectively. The developed immunosensor reaches excellent selectivity and performance characteristics to quantify biomarkers at clinically relevant values without any pretreatment. These proposed procedures could be useful to check and verify possible recurrence after clinical treatment of tumors or even report levels of disease serum biomarkers in early stages.

1. Introduction

A great challenge in medicine is to quantify specific protein biomarkers released into the blood stream or other physiological fluids for a timely and cost-effective diagnosis of both chronic and acute clinical conditions. The determination of these protein biomarkers still relies on extremely sophisticated analytical instrumentation located in centralized laboratories, because the clinical thresholds needed are typically in the femtomolar to picomolar concentration range. Therefore, there is a high need of portable and affordable point-of-care (POC) systems that can quickly and accurately quantify disease biomarkers, and this should be seen as a worldwide challenge [1,2].

Many studies have identified a number of biomarkers based on single proteins that have been successfully implemented into clinical practice [3]. A well-known disease biomarker is the prostate-specific antigen (PSA), a serine protein that has been related not only to prostate cancer but also to some female cancer in early stages. Nowadays, for clinical diagnosis or therapy evolution, PSA levels are monitored, and there are some established PSA ranges, which are referred to men with probability of suffering from prostate cancer. Total PSA values between 4 and 10 ng/mL or higher are a clear signal of prostate cancer [4], values lower than 0.1 ng/mL are a signal of satisfactory evolution of the treatment [5]. Recent research papers have shown that levels of PSA in women can be associated with breast cancer. Concentration levels around or lower than 1 pg/mL could be a signal of breast cancer in women. All these data allow us to identify to PSA as a potential biomarker for early detection, diagnosis, and prognosis of cancer in men and women [4–7]. These findings reveal the urgent need for ultrasensitive analytical methodologies able to quantify biomarkers like PSA at extremely low concentration levels to allow the use of such protein for monitoring the efficiency of the therapeutic treatment of prostate cancer and even as a useful biomarker tumor disease in women.

* Corresponding author.
** Corresponding author.
E-mail addresses: alfredo.escosura@uniovi.es (A. de la Escosura-Muñiz), soldadoana@uniovi.es (A. Soldado).

https://doi.org/10.1016/j.talanta.2024.126095
Received 1 September 2023; Received in revised form 23 February 2024; Accepted 10 April 2024
Available online 16 April 2024
0039-9140/© 2024 The Authors. Published by Elsevier B.V. This is an open access article under the CC BY-NC-ND license (http://creativecommons.org/licenses/by-nc-nd/4.0/).

During the past decade, research in nanotechnology has provided enormous opportunities for the development of ultrasensitive immunosensors. The synergic combination of the high specificity of the affinity-based interaction between antigen and antibody with the improved sensitivity, that can be achieved using nanomaterials as tags, has been successfully exploited in the development of a variety of immunosensors. Even though the advantages and huge potential of nanoparticle-based immunoassays, the detection of species requiring ultrahigh sensitivity is a challenge to their application. With the aim of improving the sensitivity of immunosensors, as well as to enhance the reading of the analytical signal, different strategies for amplification of analytical signals have been proposed based on the use of inorganic NPs. The different strategies described differ mainly in the nanoparticle detection approach: electrochemically, optically or by mass spectrometry [8–11]. When comparing the approach here developed with previously reported systems that achieve ultra-high sensitivity, some of them imply the need to include sample pretreatment steps prior to detection, such as acid digestions, the need to resort to the use of complex and expensive instrumentation (e.g. elemental mass spectrometry ICP-MS detection) or, in some cases, the need to perform controlled synthesis of nanoparticles, such as novel quantum dots QDs, that often suffer from heterogeneous size enhancements [12–16]. A smart approach that has been shown to be especially suited for such purpose makes use of an immuno-NP labelling followed by a catalytic deposition of a noble metal on the surface of the NP used as antibody tag and the final detection of the size-enlarged nanostructure. This innovative signal amplification approach is based on exploiting the catalytic properties of some inorganic nanoparticles such as Quantum Dots (QDs) or Gold Nanoparticles (AuNPs) that are able to catalyse the reduction of gold or silver ions on their nanoparticle surface selectively. Following this approach, different immunoassays based on the use of QD [12,17] or AuNPs [18,19] have been developed. Potential applicability of such approaches has been evaluated for the detection of low levels of clinical-relevant protein biomarkers, such as carcinoembryonic antigen [19] or prostate-specific antigen [17] in buffered media containing potential interferents, and also in human serum samples. Results obtained demonstrated that such approaches were suitable for clinical analysis of clinical biomarkers achieving the high demanded sensitivity. However, the sensitivity of these methods can be compromised by nonspecific metal depositions on the immunoassay support, which greatly increase the blank signals thus worsening the analytical sensitivity. To minimize such reported problems of metal chemical deposition it is noteworthy that controlled catalytic silver electrodeposition presents high specificity of the metal deposition. Using a silver electrodeposition, the metal is specifically deposited on the inorganic NP surface, thus blanks are greatly reduced due to nonspecific metal depositions. Actually, silver electrodeposition has been successfully applied for signal amplification of DNA hybridization assays and immunoassays, demonstrating both high sensitivity and selectivity [20,21].

A key parameter to be considered when developing a biosensor is the support selected to immobilize the biorecognition molecules as it affects very significantly the efficiency on the biomolecule immobilization, the stability of the sensing phase or the kinetics in the analyte recognition that, in turns, affect the final performance of the biosensor. In this context, the use of Indium Tin Oxide (ITO) as a support material for optical [22] or electrochemical [23] biosensing has grown in recent years due to its favorable properties: good electrical conductivity, high stability, efficient substrate adhesion, optical transparency, and low cost [24]. Although different strategies have been described for immobilizing biomolecules on ITO most of them are based on the formation of self-assembled monolayers (SAM) on the ITO surface, being phosphonic acids highly appropriate for such purpose due to its simple preparation, high stability, and good reproducibility [25,26].

Despite the development of numerous nanomaterial-based biosensors for PSA determination, mainly based on electrochemical and optical detection which exploit the selectivity properties of aptamers and antibodies [27], the need for low-cost and time preparation, easy-to-use, sensitive, fast and reliable diagnosis still remains. Some recent PSA sensors described in the literature require long incubation times for electrode surface modifications (taking more than 24 h), or suffer of a limited sensitivity that is not enough to reach the clinically relevant PSA concentrations that should be detected when this biomarker is intended to be used for breast cancer diagnosis [28,29]. Furthermore, decentralization of clinical tests is becoming nowadays a great need. Common diagnostic platforms and detection equipment then need to be transformed into POC systems, which must be easy-to-use, cost-effective, and portable to carry out a fast and sensitive detection by the final user. That is why synergic combination of microfluidic strategies with both electrochemical and optical detection are nowadays one of the most widely approaches used in POC sensing along with the use of nanomaterials to improve the sensitivity [30–32]. Moreover, in order not to only detect but also quantify the biomarker concentration, a good readout equipment is required. For such purpose, smartphones can be the key point as they are available to almost everyone and what is more, they are very suitable for its coupling with electrochemical and optical detection systems as well as microfluidic platforms for POC diagnostics [33,34]. Special attention has to be paid regarding potential matrix interferences that could occur with a high probability in the analysis of low levels of protein biomarkers in biological samples due to the complexity of such matrices (i.e., containing high diversity and quantities of proteins and other biochemical species). Biomarkers quantification using immunosensors (such as the work here performed) could guarantee a high selectivity degree due to the specific binding between antibodies and corresponding antigen. However, the composition of the sample matrix can still be a source of interferences affecting the detection (i.e., electrochemically or optically). This explains that, depending on the matrix sample composition, sometimes additional pretreatment steps (e.g., a previous sample dilution to minimize the influence of the matrix) must be included previous to the immunoanalysis [29,35,36].

In this work, we developed and comparatively evaluated two different analytical strategies able to quantify extremely low levels of clinical biomarkers directly in human serum, using PSA as model protein. For such purpose, an immunoassay platform was designed based on the use of a specific anti-PSA antibody immobilized onto ITO-coated polyethylene terephthalate (PET) as solid support, a AuNPs-labelled anti-PSA antibody for the recognition step, and a fast silver electrodeposition on the AuNPs tag surface before the final detection. The two analytical strategies developed mainly differ in the detection approach of the size-enhanced nanoparticle used as antibody tag. Quantification of the size-enlarged AuNPs was carried out in two different ways: electrochemically, by measuring current intensity, or optically, by using a smartphone modified with magnifying lenses as optical detector. The proposed strategies are easy to use and low-cost methodologies that can be applied to quantify other biomolecules just by simply selecting a set of different antibodies adapted to the desired target molecules.

2. Materials and methods

2.1. Reagents and materials

All reagents used were of analytical grade and used as received, without any further purification, unless stated the contrary. 6-phosphonohexanoic acid (PHA), hydrogen peroxide (H_2O_2), ammonium hydroxide (NH_4OH), bovine serum albumin (BSA), casein from bovine milk, silver nitrate ($AgNO_3$), N(3-Dimethylaminopropyl)-N′-ethylcarbodiimide hydrochloride (EDC), N-hydroxysuccinimide (NHS), Tween 20, Anti-Rabbit IgG−Peroxidase antibody (A8275), Anti-Mouse IgG−Peroxidase antibody (A3673), and 3,3′,5,5-tetramethylbenzidine (TMB) liquid substrate solution were obtained from Sigma-Aldrich (Germany). Carboxylated-gold nanoparticles, 20 nm diameter, were purchased from Nanovex Biotechnologies (Spain). Rabbit polyclonal

anti-PSA (ref. ab19554), mouse monoclonal anti-PSA (ref. ab403), and prostate-specific antigen (ref. ab78528) were obtained from Abcam (UK). Indium tin oxide coated polyethylene terephthalate (ITO-PET) sheets (surface resistivity 60 Ω/sq) were purchased from Sigma-Aldrich (Spain). The electrochemical transducers were ITO-PET pieces of 40 × 20 mm, where a working area of 8 mm in diameter is defined with a translucent plastic adhesive washer (APLI, Spain) made of polypropylene with a hole diameter of 8 mm, by simple assembling it on the ITO-PET surface.

All solutions were prepared with deionized ultrapure water (18.2 MΩ cm) that was obtained with a PURE LAB flex3 from ELGA Labwater (UK). Electrochemical measurements were carried out with 1 mM silver nitrate solution in 1 M NH_3, prepared in deionized ultrapure water, and at room temperature.

2.2. Instrumentation

An UV–Vis Spectrophotometer Genesys 10S from Thermo Scientific (Germany) and a laser confocal microscope spectra Leica TCS-SP2-AOBS from Leica microsystems (Germany), with a 63-oil immersion objective, were used to characterize AuNPs and optimize their enhancement. A Helium-Neon 543 nm laser (5 mW) was employed at 35 % to irradiate microscope slides with ITO sheets attached. Laser confocal microscope was used in reflection mode to visualize the particles obtained after the silver enhancement step.

Electrochemical measurements using ITO electrodes were carried out by using a methacrylate cell with a 400 μL well and a three-electrode system with the ITO-PET working electrode, a silver/silver chloride reference electrode from CH Instruments, Inc. (USA) and a platinum wire counter electrode from Alfa Aesar (USA). The electrochemical measurements were performed by using an EmStat3 Blue potentiostat from PalmSens (The Netherlands) controlled via Bluetooth with a smartphone through PStouch app (for Android mobile operative system). The experimental set-up is shown in Fig. 1.

DIPLE® device, consisting on Fine Stage and magnifying lenses with a spatial resolution between 0.7 and 0.8 μm from SmartMicroOptics (Italy), was coupled to a smartphone (Samsung Galaxy A5 with a frontal camera of 16 megapixels) to acquire the images of the silver size-enhanced structures and carry out the optical detection. This device is an easy to use, compact and portable kit that transforms any smartphone or tablet into a powerful optical microscope.

2.3. Procedures

In this work, we have developed two different strategies to detect and quantify PSA. Both methodologies are based on the electrocatalytic deposition of silver onto AuNPs surface. Final detection can be carried out by measuring current intensity or number of enhanced structures using a portable potentiostat or a magnifying lens coupled to a common smartphone (see Fig. 1).

Noncompetitive immunoassay formats (usually the sandwich-type formats) give the highest level of sensitivity and specificity because of the use of a couple of match antibodies. The measurement of a labelled antibody is directly proportional to the amount of antigen present in the sample, thus resulting that the detectable signal increases with the increasing target analyte. Therefore, sandwich-type assay is today one of the most popular immunosensing schemes for protein biomarkers detection. In this work we used a capture antibody and an AuNP labelled antibody in the design of a sandwich-type immunoassay for recognition and detection the protein biomarker PSA. The first one (capture antibody) was a polyclonal protein able to recognize more than one epitope thus, ensuring a high efficiency in recognition of PSA analyte by the immobilized capture antibody, avoiding steric impediments. Specificity and sensitivity are then achieved by using a monoclonal nanoparticle-labelled antibody".

2.3.1. Antibody:AuNPs bioconjugation

Commercial carboxylated 20 nm-AuNPs were functionalized with monoclonal anti-PSA antibody by using the EDC/NHS carbodiimide-mediated hapten-carrier conjugation reaction. A labelled monoclonal protein was used in order to ensure the specificity of the proposed immunoassay. The protocol carried out was as follows: 100 μL of carboxylated AuNPs were incubated with 100 μL of EDC/NHS solution (1 mg/mL EDC and 2.5 mg/mL NHS) in 10 mM pH 7.4 phosphate buffer (PB) for 30min at room temperature. After that, the mixture was centrifuged at 7500 g for 30min to eliminate the excess of unreacted EDC/NHS. The obtained pellet was re-suspended in 10 μL of monoclonal antibody solution (1 mg/mL). This mixture was incubated for 2 h and then 10 μL of BSA solution (1 %) was added to block the non-covered surface of AuNPs. After 30min of incubation, the mixture was centrifuged for 15min at 4000 g to purify the bioconjugate. Finally, the pellet was re-suspended in PBS 10 mM with Tween 20 at 0.01 % as preservative. The absorption spectra of AuNPs and bioconjugates (AuNPs:Ab) were collected and detailed in Fig. S1. As it can be seen, the optical properties of the AuNPs are preserved after bioconjugation.

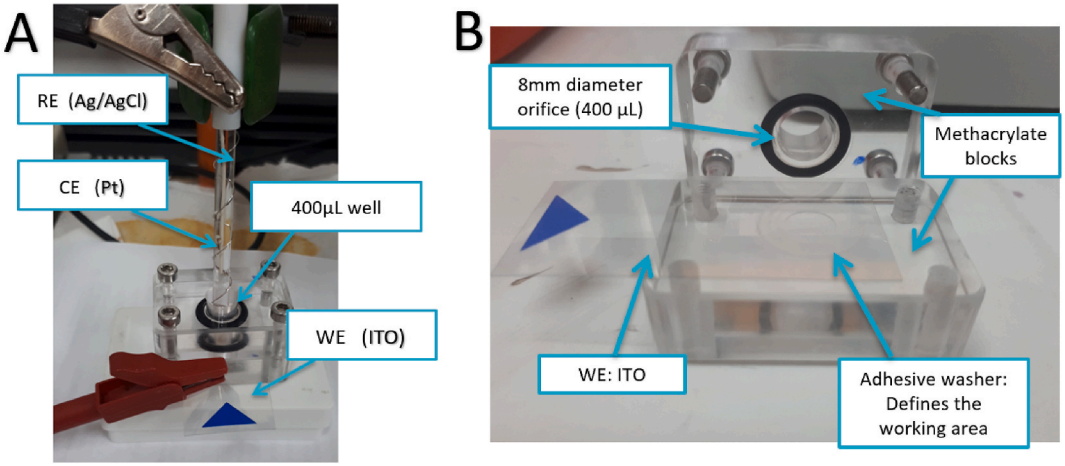

Fig. 1. A) Assembly of the electrochemical cell, formed by an ITO working electrode (WE), Ag/AgCl reference electrode (RE) and Pt counter electrode (CE). B) Components that define the electrochemical cell, composed of two methacrylate blocks and the ITO piece, where the working electrode area is defined with an adhesive washer, serving the rest of the sheet as electrical connection piece.

2.3.2. Sandwich-type immunoassay for PSA detection using AuNP tags and silver electrodeposition

First, the surface of the ITO-PET electrode must be activated for further immobilization of the capture antibody, a polyclonal protein which is able to recognize more than one epitope, ensuring the attachment of PSA to the immunoplatform. This was achieved by following a previously reported protocol [2] (see detailed protocol in Supplementary information). After the surface activation, an adhesive washer was used to define in the activated ITO sheet a working area of 8 mm in diameter and 0.2 mm height. Then, 30 μL of EDC/NHS solution (1 mM) was added to the working area for activation of the carboxyl groups of the phosphonic acid-modified ITO and incubated at 37 °C for 30min. After that, the EDC/NHS solution was removed and 30 μL of 4 μg/mL of capture antibody solution (rabbit polyclonal anti-PSA) were dropped in the well and incubated at 37 °C for 6 h. Finally, the solution was removed, and the surface was blocked by incubating the well with 30 μL of casein solution (1 %) in PBS overnight at 4 °C.

After the blocking step, wells were washed three times using the washing solution (WS) consisting on 30 μL 10 mM PBS pH 7.4 in 0.05 % Tween 20. Next, 30 μL of the samples (containing PSA) were added to previously assembled wells and were incubated for 2 h at 37 °C [14,17]. Then, another washing step with the WS was performed. Continuing with the immunoassay, 30 μL of 1 μg/mL of the secondary antibody labelled with the AuNPs (prepared as described in section 2.3.1) were deposited and incubated 1 h at 37 °C. Finally, after removing the solutions, a washing step with deionized water was carried out. A controlled silver electrodeposition on the surface of the AuNPs used as antibody tags was carried out after formation of the immunocomplex and before the NP tag detection. It should be highlighted that the NPs size enhancement is dependent on the size of the AuNPs tags. In fact, as previously described [37], the catalytic activity of gold nanoparticles is higher for those AuNPs with smaller sizes. Thus, here we selected 20 nm-AuNPs in order to warranty a high catalytic activity while ensuring a high colloidal stability and an efficient labeling of antibodies [17], that means, having an elevated number of detectable AuNPs per antibody to achieve a maximum sensitivity. For such purpose, the electrochemical cell is assembled with the ITO-PET sheet in which the immunoassay was performed (see Fig. 1) and 400 μL of an amplification solution containing 1 mM $AgNO_3$ in NH_3 1 M were added. The amount of electrodeposited silver, at a controlled potential, is proportional to the number of AuNPs on the electrode surface. Consequently, the re-oxidation peak produces a current proportional to AuNPs quantity. This process is highly effective due to the large surface area of AuNPs which allows an easy diffusion and reduction of the silver ions, forming a metallic silver layer onto the AuNP surface (electrochemical detection). Finally, an oxidation sweep was performed directly to re-oxidize the silver into silver ions and achieve the produced current signal (electrochemical detection) or a gently washing step with deionized water was performed before the smartphone optical detection, of the generated microstructures (smartphone optical detection). A scheme of the sandwich-type immunoassay process is shown in Fig. 2. It should be highlighted that in this assay the silver electrodeposition step on the surface of the AuNPs takes place at the end of the immunoassay (i.e., after the formation of the immunocomplex) and before the size-amplified NP detection. For this reason, any possible effect that the silver electrodeposition procedure may have on the activity of the antibodies will not affect the final assay.

2.3.3. Quantitative processing of smartphone pictures

Once completed the immunoassay and the selective silver electrodeposition on the AuNPs, the ITO-PET sheet was placed on the DIPLE® device. Fig. 3 shows the DIPLE® fine stage and magnifying lenses with a spatial resolution between 0.7 and 0.8 μm from SmartMicroOptics (Italy), that were coupled to the Smartphone (Samsung Galaxy A5 with a frontal camera of 16 megapixels) to acquire the images of the silver size-enhanced structures. By shifting the scroll wheel in the DIPLE device, different zones of the ITO surface were photographed (10 images per well), and a total surface of 0.06 mm^2 is scanned per sample. The time required to complete such an analysis is below 5 min. Once the images were taken, they were processed using the open source "ImageJ" Java-based image processing program, with a wide availability of user-written macros and plugins. A customized compilation of the ImageJ program (named Confocal Uniovi ImageJ), designed by the Photonic Microscopy and Image Processing Unit of the University of Oviedo (Spain), has been used to process all the acquired pictures. This compilation includes several functions and plugins with the main objective of processing optical microscopy images. To facilitate the microstructure counting in the images, a macro has been created, based on a simple code that allows selecting, discriminating, and counting the structures in each image. The macro performs an automatic search loop of all images stored in a folder, and it opens image by image, allowing to work with several pictures at the same time. Interactively, the user selects the enhanced structures, and the macro registers the number of particles per image, allowing discrimination of artifacts. Finally, once the counting step is finished, the macro exports a text file with the results of the measurements and ends the process loop. The signal obtained for each image (i.e., the number of particles) is then related to the PSA concentration in the sample by an external calibration. To do that, a concentration-response curve (number of microstructures *vs.* PSA

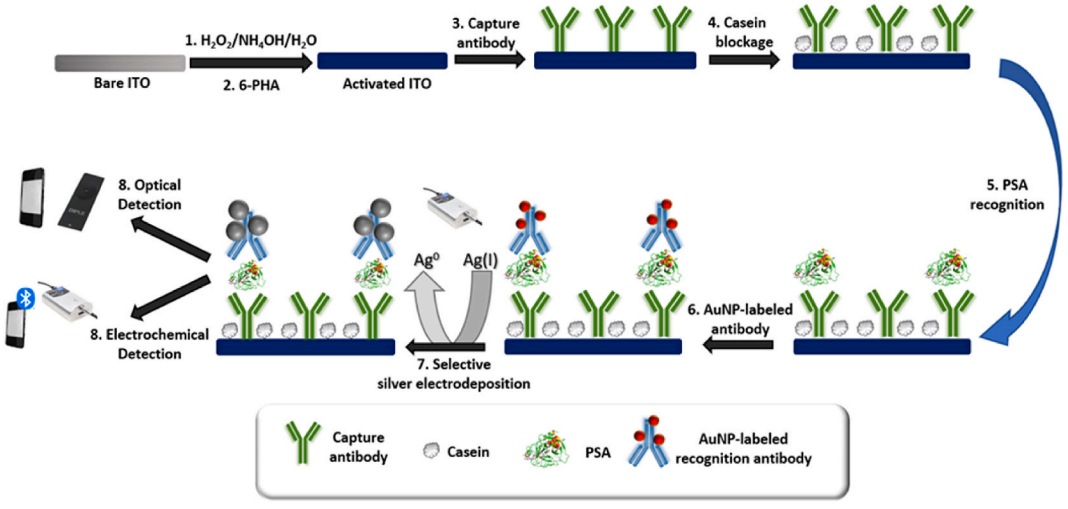

Fig. 2. Scheme of the immunoassay developed to detect prostate-specific antigen (PSA) using AuNPs antibody-tags and controlled silver electrodeposition on the AuNPs surface for signal amplification.

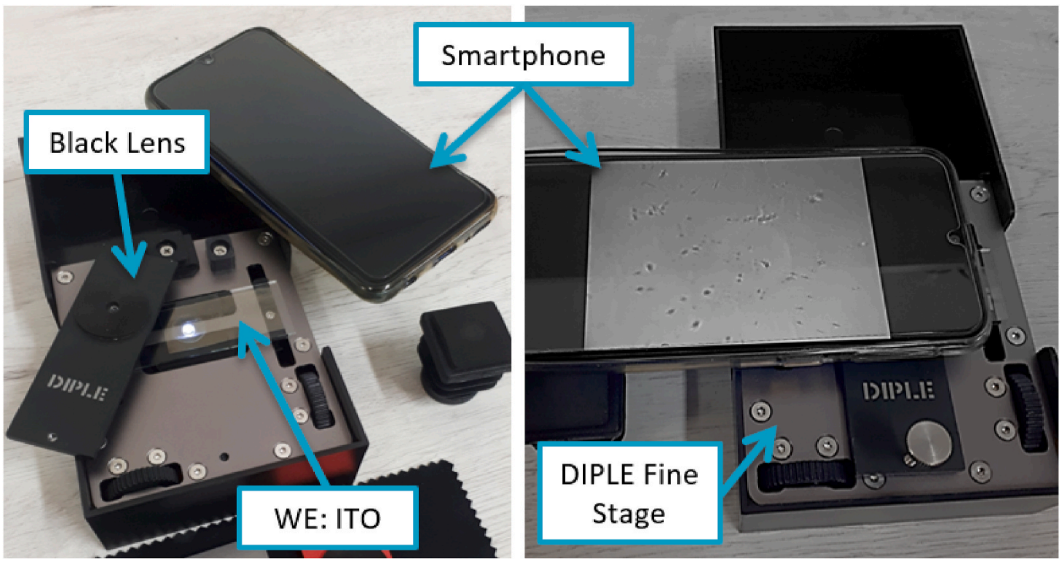

Fig. 3. DIPLE® device and lenses employed for optical detection with a smartphone.

concentration) was obtained by analyzing several standard buffered solutions of known PSA concentration with the proposed immunoplatform.

3. Results and discussion

This designed sensing system based on controlled silver electrodeposition presents several advantages over other previously reported chemical reduction procedures such as a higher signal to noise ratio and the reduction of unspecific silver depositions [38]. The following sections show a detailed description of the optimized parameters and results obtained to quantify PSA using a dual-mode detection procedure.

3.1. Electrocatalytic deposition of silver on AuNPs

Firstly, we studied the possibility to achieve silver deposition onto the surface of the AuNPs upon reduction of the silver ions from the amplification solution, to obtain an enhancement of the size of the NPs used as tags of the immunoassays. As mentioned in the introduction section, catalytic gold or silver chemical deposition on different types of inorganic nanoparticles has been successfully proposed [12,17–19]. However, such chemical reduction procedures often suffer from nonspecific metal depositions on the support employed for the immunoassay. Alternatively, here we tested the possibility to perform a catalytic electrodeposition of silver on the surface of the AuNPs used as tags in the detection anti-PSA antibodies.

In this idea, the electrocatalytic activity of AuNPs toward the silver electrodeposition was first evaluated by cyclic voltammetry (Fig. S2). Scans from +0.40 to −0.80 V were recorded, in an aqueous 1.0 M NH_3/ 1.0 mM $AgNO_3$ amplification solution, using an activated ITO-PET electrode without AuNPs (green) and an activated ITO-PET electrode with AuNPs previously adsorbed during 15min (red). It can be observed that the half-wave potential of the silver reduction process is shifted to less negative potentials (ΔE around 150 mV) when AuNPs are previously deposited on the electrode surface. This means that, ensuring an adequate deposition potential, i.e. −0.02 V, the electroreduction of silver ions takes place specifically on the AuNPs rather than on the electrode surface (see Fig. S2). This process is highly effective due to the large surface area of AuNPs, which allows an easy diffusion and reduction of the silver ions, forming a metallic silver layer onto the AuNP surface (Equation (1)). Moreover, once a layer of silver is formed, silver ions are reduced on the silver shell due to a self-enhancement deposition. After silver reduction onto AuNPs surface, a positive potential sweep in the same medium was applied to produce the re-oxidation of silver (Equation (2)).

$$Ag(NH_3)_2^+ + 1e^- \xrightarrow{AuNP, E=-0.02V} Ag^0\ (deposited\ on\ AuNPs) + 2NH_3$$

[Equation 1]

$$Ag^0\ (deposited\ on\ AuNPs) + 2NH_3 \xrightarrow{E\ (-0.02V\ to +0.3V)} Ag(NH_3)_2^+ + 1e^-$$

[Equation 2]

In order to find the best experimental conditions for the electrochemical deposition of silver onto the AuNPs surface several studies were done. Firstly, different concentrations of silver nitrate in the enhancement solution (from 0.2 to 5 mM $AgNO_3$) were tested. Higher $AgNO_3$ concentrations resulted in a faster Ag(I) diffusion into the ITO surface where AuNPs are deposited. However, as a compromise between an efficient Ag electrodeposition on the AuNPs and looking forward to ensure a good selectiveness (minimize unspecific depositions), 1 mM $AgNO_3$ was selected for further studies.

After selecting silver concentration of the deposition solution, different potentials in the range from −0.1 to −0.01 V were evaluated (see supplementary information, Fig. S3). The optimum potential found for efficient Ag deposition on the AuNP surface was −0.02 V, as it provides the best signal to noise ratio among tested potentials. Finally, the deposition time was also studied from 5 to 40s, being 20s the appropriate time as it was the one producing the larger microstructures in the shorter time as well as presenting the lowest backgrounds between the different deposition times evaluated (see Figs. S4 and S5). These optimized conditions minimize eventual unspecific Ag depositions on the ITO surface, bringing on the enhancement of AuNPs size from nano to micrometer structures, easy to be observed with DIPLE lenses. In addition, the optimized conditions bring to a controlled electrochemical catalytic deposition, resulting in a highly homogeneous NP size-enhancement to the micrometer scale with a very similar shape pattern. This constitutes an important achievement of the here proposed approach being a critical aspect in the performance of the biosensor.

Summarizing, selected conditions to attempt this work were as follows: −0.02 V as deposition potential, 20s for electrodeposition time and 1 mM for the $AgNO_3$ concentration in the enhancement solution.

3.2. Development of the silver amplified PSA immunoassay

The developed “silver amplified” immunoassay procedure consists on the immunoreaction of the antigen (PSA) with the capture antibody

(adsorbed on the surface of the modified ITO-PET surface) and then the reaction with an appropriate AuNPs labelled detection antibody to form a sandwich complex. The size of the AuNPs used as tags of the detection PSA antibody was then amplified using the silver electrodeposition as previously described (see section 3.1). A portable potentiostat was employed for electrochemical measures and a smartphone coupled to a lens system was used to visualize the obtained Ag enlarged nanostructures (see Figs. 1 and 3 respectively). Fig. 4 shows the AuNPs before and after catalytic silver electrodeposition. As can be seen in Fig. 4, generated microstructures have sizes of few μm, and look like little stars or nanospheres with spicules that allows a better discrimination between the enhanced-nanostructures and potential artifacts that could eventually be present in the immunoplatform surface.

As customary, the concentration of the capture antibody, the concentration of Ab:AuNPs bioconjugate and the blockage methodology were firstly optimized, being the optimal conditions: 4 μg/mL:1 nM (Ab:AuNPs) and casein 1 % respectively (see Figs. S6, S7 and S8 of the Supporting Information).

To evaluate quantification parameters and the success of the procedure, the proposed immunoassay was carried out with different PSA concentrations and both electrochemical and optical responses were evaluated. For the electrochemical detection, PSA concentrations assayed were ranged between 10 pg/mL and 10^4 pg/mL, and as can be seen in Fig. 5, the current increases with PSA concentration. When plotting Intensity versus the logarithm of PSA concentration, a linear response was obtained, with a regression coefficient of 0.962.

As shown in Fig. 5 a shift in the silver re-oxidation peak toward more positive potentials is observed, which agrees with a common behavior previously observed in systems using external reference electrodes [20]. It must be taken into account that, in the NP-based sandwich-type immunoassay, an increase in the analyte (PSA) concentration results in a higher number of NPs to be detected and, therefore, the amount of electrodeposited silver is higher. As a consequence, the re-oxidation of the reduced silver deposited on the AuNPs, required for its quantification, will be less efficient and irreproducible, thus explaining the higher standard deviation of signals observed at higher PSA concentrations. As the main objective of this approach is the quantification of very low concentration levels of PSA (i.e., lower than 1 pg/mL, the clinically relevant level for breast cancer), the high standard deviation of signals observed at high PSA concentrations cannot be considered as a limitation of the approach. When samples containing high PSA levels must be analyzed, quantification can be done just by carrying out a previous sample dilution.

In order to carry out the optical detection, the number of silver-enhanced AuNPs on the ITO electrode were visualized with the optical system showed in Fig. 3. The microstructures generated were visualized by simply placing the immunoplatform on the DIPLE device and focusing the lens with the smartphone. Results obtained after analyzing standards ranged between 1 pg/mL to 10^4 pg/mL are shown in Fig. 6. Representative images resulting from silver-amplified structures when increasing PSA concentrations are shown in Fig. 6A. When assaying different PSA concentrations, the number of structures that are observed increases gradually with the PSA concentration. For each well, the total number of structures measured for a given PSA concentration was computed as the sum of 10 representative images that were taken in different zones of the same well, avoiding the borders. The number of silver-enlarged structures in each image was computed with the ImageJ macro designed for this work (see 2.3.3 Section, Quantitative Processing of Smartphone Pictures). When plotting the average number of particles observed in 3 different wells of the same PSA concentration *versus* PSA concentration, a typical dose-response immunoassay curve was observed (Fig. 6B). It must be taken into account that, even though both the electrode surface and the gold nanoparticle-labelled antibodies are blocked (with casein and BSA solutions respectively) to avoid unspecific absorptions, always a small amount of undesirable protein (in our case, the gold nanoparticle-labelled antibody) is adsorbed on the electrode surface. This explains that a few microstructures are detectable in the blank assays, in the absence of the analyte, (Fig. 6Aa). This is commonly observed in conventional immunoassays, as extensively reported in the literature [20,39,40]. This blank value has been considered in the calibration plot. The ten images representing the analyzed well corresponding to Fig. 6 are shown in the Supplementary Information (from Fig. S9 to Fig. S13). Table S1 in the supplementary information section collects the data used to calculate equation (3), limit of detection (LOD), limit of quantification (LOQ) as well as the blank signal value and its standard deviation and RSD for each concentration measured. These results were linearized, by plotting the number of structures *vs.* the logarithm of the PSA concentration (Fig. 6C), obtaining a fitted equation (Equation (3)) with a regression coefficient of 0.994.

$$N^{o}\ of\ particles = 51.3\ \ln[PSA] + 191.7 \qquad \text{[Equation 3]}$$

To carry out the calculation of the detection limit, the PSA response curve shown in Fig. 6B (typical of conventional immunoassays) has been linearized plotting the PSA concentration on a logarithmic scale. The data from the normal-log dose-response curve obtained now fit to a normal distribution. Then, the IUPAC criterion (3σ criterion) can be applied to calculate the LOD of the assay by using the calibration equation of Fig. 6C (Equation (3)) and the signal deviation of the blanks [41,42]. LODs and LOQs for both calculations resulted in 37 and 102 fg/mL of PSA for optical and electrochemical LODs respectively and being 64 and 1183 fg/mL of PSA for optical and electrochemical LOQs respectively. The high sensitivity achieved for PSA detection makes the proposed immunosensors and more remarkably the optical detection, helpful for women's breast cancer diagnosis, because recent studies have suggested that PSA could act as a biomarker, being a normal woman serum level around 1 pg/mL, which is typically undetectable by using standard assay methods. Furthermore, the calibration curve shown in Fig. 6 suggested that the designed immunoplatform exhibits a linear

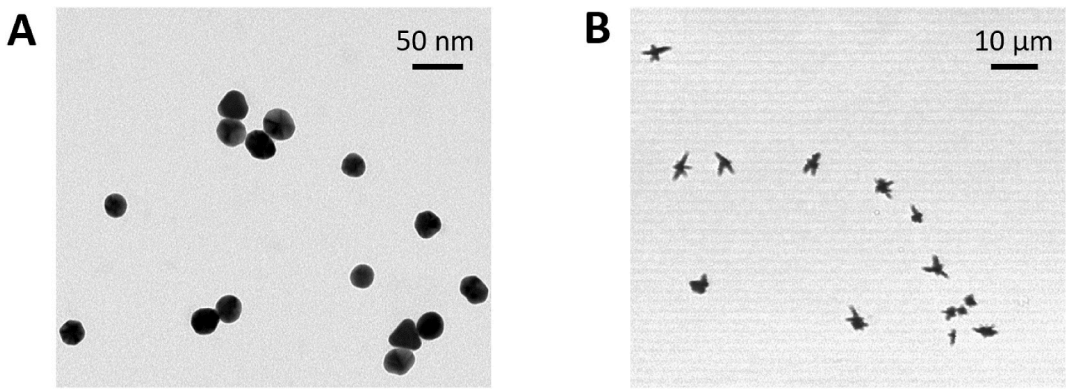

Fig. 4. A) TEM image of AuNPs before silver enhancement. B) Confocal microscopy image of the microstructures generated after AuNPs silver enhancement.

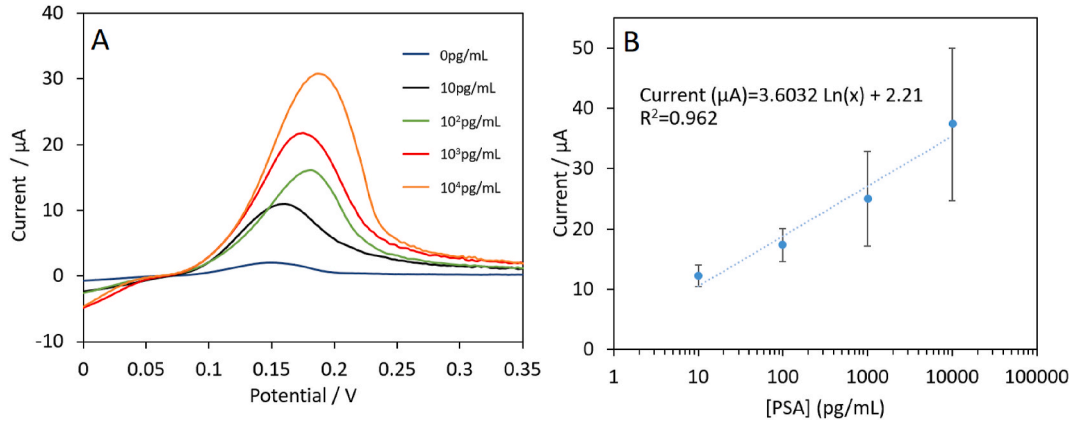

Fig. 5. Electrochemical detection: A) Oxidation sweeps after carrying out the immunoassay for given PSA concentrations, scanned from −0.02 V to +0.35 V in aqueous 1.0 M NH_3 - 1 mM $AgNO_3$. Silver deposition potential: −0.02 V; silver deposition time: 20s; scan rate: 50 mV/s. B) Relationship between PSA concentrations and obtained silver oxidation peak currents.

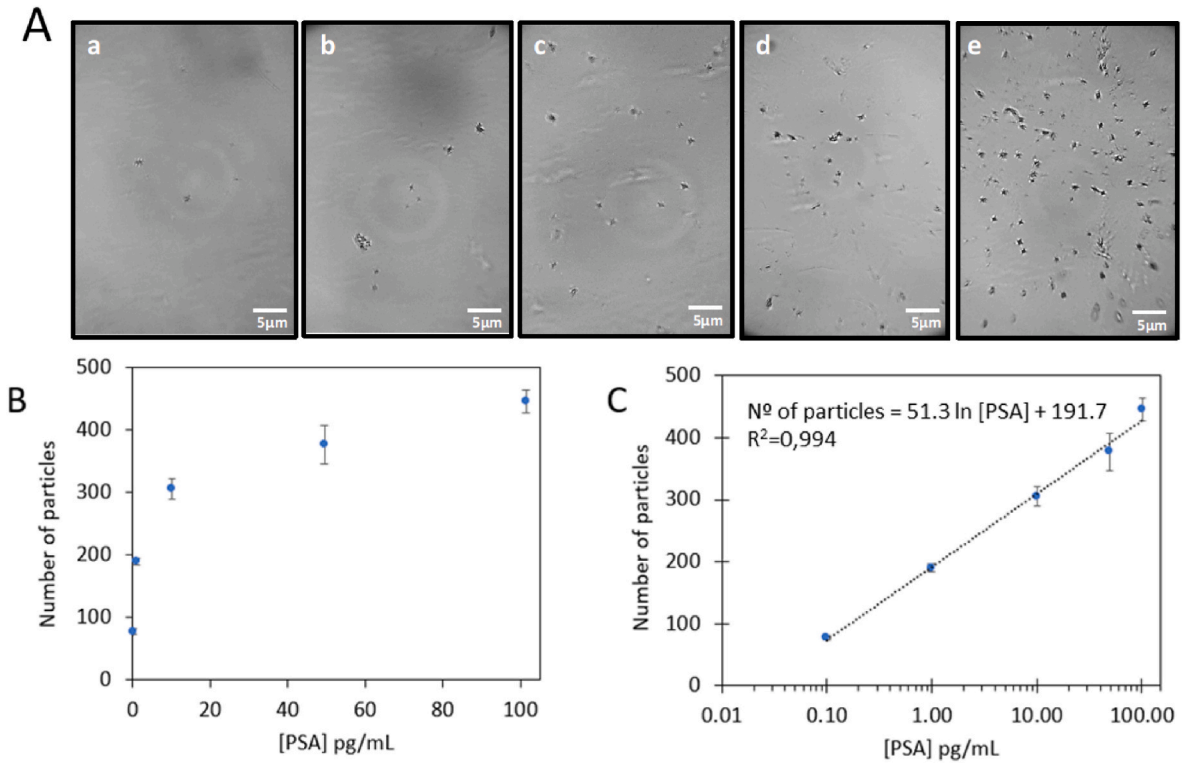

Fig. 6. A) Images of the immunoplatform taken with the smartphone after carrying out the immunoassay and the catalytic silver electrodeposition for several PSA concentrations: a) 0, b) 1, c) 10, d) 50 and e) 100 pg PSA/mL; B) Immunoassay curve obtained plotting the number of microstructures obtained at different PSA concentrations C) Immunoassay response plot, linearized by applying log to the X-axis scale, obtained after image processing of silver-enhanced AuNPs smartphone images at the different PSA concentrations.

dynamic range of at least up to 100 pg/ml PSA (maximum concentration PSA assayed, which is two orders of magnitude above the clinically relevant level required to be quantified when such biomarker is used for breast cancer diagnosis). Precision of the methodology was assessed by evaluation the RSD (n = 3) of the signals obtained for the quantification of a 1 pg/mL PSA concentration, obtaining a value as good as 3 % for the optical detection. For the electrochemical detection, 10 pg/mL was the concentration tested to assess the precision of the approach, obtaining a value of 14 % for the RSD.

Results obtained using electrochemical and optical detection are summarized in Table 1. When comparing analytical signals and RSD values obtained using both procedures, for the analysis of samples containing the same PSA concentrations (i.e. 0, 10 and 100 pg/mL), the lowest RSD values were obtained for the optical approach (i.e., electrochemical NP-size enhancement followed by an optical detection of the enlarged nanostructure). Related with analytical performance, an enhancement of the sensitivity is observed for the optical detection, reaching a LOQ almost 20 times higher than the one obtained by an electrochemical detection.

For comparison purposes, Table 2 summarizes the analytical performance characteristics reported for some of the biosensors for PSA quantification based on the use of nanomaterials developed so far. The method here proposed for PSA quantification greatly satisfies the sensitivity requirements for analysis of clinical samples containing

Table 1
Comparison between detection signals and analytical performance of proposed approaches for PSA quantification.

	Electrochemical approach		Electro-optical approach	
[PSA] pg/mL	Signal (μA)	RSD (%)	Signal (number of particles)	RSD (%)
0	2.0	18	77	5.4
10	12.2	14	306	5.3
100	17.3	15	445	4.1
Analytical Performance				
	[PSA]		[PSA]	
Lineal Range	$10–10^4$ pg/mL		$1–10^2$ pg/mL	
LOD (fg/mL)	64		37	
LOQ (fg/mL)	1183		102	

RSD: Relative Standard Deviation; LOD: Limit of Detection; LOQ: Limit of Quantification.

protein biomarkers at extremely low concentration levels. The immunoplatform developed, which incorporates an electrochemical NP-size enhancement followed by an optical detection of the resulting enlarged nanostructures using a smartphone, can be employed in combination to a portable potentiostat, thus allowing to detect the biomarkers at POC. The obtained LOD (37 fg/mL) is lower than the values reported for other similar bioassays described for PSA detection that incorporate a signal detection also compatible with of low-cost or portable instrumentation (e.g. Horseradish Peroxidase (HRP)-Absorbance (4×10^5 fg/mL) [43], Mn-Zn QDs Phosphorescence (17×10^3 fg/mL) [14], Upconverting Nanoparticles (UCNS)-Fluorescence (1×10^4 fg/mL) [28], Au-NPs–electrochemical (28×10^3 fg/mL) [29] or AgNP-SERS (1×10^5 fg/mL) [36]). Particularly, when compared to other smartphone-based methodologies recently described [33], the here-reported platform displays a detection limit for PSA quantification that is two orders of magnitude lower.

One of the drawbacks of the technique here described could be its somewhat lengthy analysis time, which is mostly attributable to the 2-h incubation and 1-h recognition steps. In any case, this inconvenience is similar to other reported procedures (see Table 2), with the exception of the approach based on Au-nanospears [44] that require a total time of less than 1 h for both incubation and recognition steps. Some other alternative detection techniques, such as elemental mass spectrometry (ICP-MS) [12] or Confocal Microscopy [17] also provide very low detection limits for PSA detection, but require the use of expensive centralized laboratory instrumentation and trained personnel.

Alternatively, label-free and direct methodologies have been also proposed to quantify PSA, which do not need an extensive preparation or amplification step with NPs. These assays are fast and selective; however, sensitivity is limited as compared with those approaches using nano-tags that have demonstrated their usefulness to greatly improve the analytical signal [45,46]. As recent representative examples, detection limits reported for label-free PSA biosensors ranges from 10^4 fg/mL as reported by Liu et al. [45] or 2.8×10^5 fg/mL described in the work from Argoubi et al. [46], that are clearly unfavorable compared with the LOD obtained with the here reported approach based on NP-labelled antibodies (i.e. 37 fg/mL). In addition, these label-free assays typically rely in the use specific aptamers that can suffer degradation in biological medium probably due to the interaction with nucleases. The generation of aptamers in most cases needs highly purified molecules, which is a time-consuming procedure. Moreover, sometimes aptamers synthesized with prokaryotic cells do not recognize eukaryotic proteins [47].

3.3. PSA quantification in human serum samples: spike and recovery

The applicability of the designed immunosensor for PSA was evaluated by determining total PSA levels in real serum samples from healthy women. Serum was separated from blood samples (provided by volunteers, anonymously and without profit) in a clinical center following the Standard Operational Procedures. Collected serum samples were kept frozen until use. Analysis of healthy women's serum by the proposed methodology resulted in undetectable PSA levels (below the LOD). Therefore, validation of the proposed methodology, and assessment of the eventual influence of other possible coexistent species in the samples, was performed by analyzing such serum samples spiked with known PSA concentration levels (Internal Reference Material). For such purpose, real healthy women serum was directly spiked with PSA at final concentration levels of 2 and 20 pg/mL (i.e., relevant concentration ranges in the early diagnosis of diseases, such as breast cancer, where the PSA concentration levels to be detected are extremely low). Spiked samples were prepared adding a minimum volume (5 and 50 μL) of PSA standard solution (200 pg/ml) directly to 500 μl of serum without any

Table 2
Analytical characteristics of different strategies developed for PSA detection incorporating a signal amplification step.

Analytical tag	Amplification step	Detection technique	Assay format	Dynamic range (pg/mL)	LOD (fg/mL)	Ref.
HRP	Enzymatic	Absorbance	Sandwich immunoassay	$10^3–5 \times 10^3$	4×10^5	[43]
Mn-ZnS QDs	Nanoparticle-enhanced sensitivity	Phosphorescence	Sandwich immunoassay	$50–2.4 \times 10^5$	17×10^3	[14]
Mn-ZnS QDs	Catalytic gold deposition	ICP-MS (Au)	Sandwich immunoassay	$10^{-3}–10^4$	26×10^{-3}	[12]
Mn-ZnS QDs	Catalytic gold deposition	Reflection confocal microscopy	Sandwich immunoassay	0.01–100	1.1	[17]
UCNPs and AuNPs	Upconversion enhancement	Fluorescence	Sandwich immunoassay	$100–10^3$	10^4	[28]
AuNPs	Nanoparticle-enhanced sensitivity	Electrochemical	Aptamer-based assay	34–57	28×10^3	[29]
Au-nanospears	Nanoparticle-enhanced sensitivity	Electrochemical	Aptamer-based assay	$12.5–20 \times 10^4$	50×10^3	[44]
Magnetic microbeads	Enzymatic	Electrochemical	Sandwich immunoassay	10–1500	2×10^3	[33]
AgNPs	SERS	Electrochemical	Aptamer-based assay	$100–2 \times 10^4$	1×10^5	[36]
AuNPs	Catalytic silver deposition	Direct optical detection with smartphone	Sandwich immunoassay	1–100	37	This work
AuNPs	Catalytic silver deposition	Electrochemical	Sandwich immunoassay	10–1000	91	This work

HRP: Horseradish Peroxidase; QDs: Quantum Dots; UCNPs: Unconverting Nanoparticles; NPs: Nanoparticles; SERS: Surface-Enhanced Raman Spectroscopy; ICP-MS: Inductively Coupled Plasma Mass Spectrometry; LOD: Limit of Detection.

dilution of the initial serum, followed by proper homogenization. Further, these spiked serums were analyzed following the described immunoassay with optical detection. A blank sample (healthy women serum media without any PSA spike) was also analyzed. The total amount of PSA present in the spiked serum samples was quantified employing a dose response curve obtained using standards of the protein dissolved in PBS buffer, as previously described.

Images of the immunoplatform acquired with the smartphone after the immunoassay and the silver electrodeposition on the AuNPs tags are shown in Fig. S14. The presence of possible interfering proteins or other species present in the serum samples did not induce any detectable enhancement or attenuation of the optical signal and did not produce detectable negative effects in the formation of amplified silver-enlarged structures.

After applying the calibration curve, the experimentally obtained quantitative PSA results for the different well zones of the spiked sample are collected in Table 3 and were very close to the theoretical values in the samples assayed: 1.8 ± 0.1 pg/mL PSA and 21.5 ± 0.1 pg/mL PSA (quantitative recoveries of 91 % and 107 %). These experimental results have already demonstrated that the proposed procedure allows discriminating among close concentration levels providing a reliable classification of the samples when the patients are healthy or diseased. Such quantitative recoveries confirm that sample matrix composition does not introduce any interference effect that could affect the reliability of the immunoassay, thus certifying the high selectivity of the proposed methodology for PSA quantification at extremely low concentration levels in real human serum analysis.

4. Conclusion

Here, an analytical signal amplification strategy, based on a controlled electrocatalytic silver deposition on AuNPs surface, has been optimized and integrated into a nanoparticle-based sandwich-type immunoassay for highly sensitive detection of a protein biomarker (PSA). The proposed strategy resulted in a huge and homogeneous increase of the size of the AuNPs used as antibody tags, thus making them visually detectable just by using a smartphone, and also resulting in a higher amount of electrochemically detectable silver atoms.

The immunoassay combines two steps, a PSA immunorecognition and the antibody label detection (i.e., Ag size-amplified AuNP) based on an electro-optical approach. The first one, immunorecognition, lasts 3 h and the second one, electrochemical amplification plus detection, no more than 3min, resulting in a total analysis time of about 3 h. Two detection systems, electrochemical and optical, of the Ag size-amplified AuNPs were compared obtaining the best analytical performance when carrying out an optical detection (LOD of 37 fg PSA/mL). The developed approach allows the direct quantification of low levels of PSA in human serum samples, without any sample pre-treatment, obtaining good analyte recoveries (91–107 %).

Finally, the immunoplatform can be used in combination to a portable potentiostat that can be connected to a smartphone allowing performing both the control of the electrodeposition process and the final NP-enlarged detection, thus making feasible the detection of biomarkers at POC. Moreover, the proposed procedure can be tailored to sensitive quantification of other different biomarker of interest just by simply changing the capture and the AuNPs-labelled recognition antibodies.

CRediT authorship contribution statement

Guillermo Redondo-Fernández: Writing – original draft, Methodology, Investigation, Data curation. **Laura Cid-Barrio:** Methodology, Investigation. **María T. Fernández-Argüelles:** Methodology, Conceptualization. **Alfredo de la Escosura-Muñiz:** Writing – review & editing, Supervision, Methodology, Conceptualization. **Ana Soldado:** Writing – review & editing, Supervision, Conceptualization. **José M. Costa-Fernández:** Writing – review & editing, Supervision, Methodology, Funding acquisition, Conceptualization.

Table 3
PSA quantification and recovery assay data for woman serum spiked samples.

Spiked PSA Concentration	Estimated PSA Concentration	Recovery (%)
2 pg/mL	1.8 ± 0.1 pg/mL	91
20 pg/mL	21.5 ± 0.1 pg/mL	107

Declaration of competing interest

The authors declare the following financial interests/personal relationships which may be considered as potential competing interests: Guillermo Redondo-Fernández reports financial support was provided by Spanish Ministry of Science and Innovation. Guillermo Redondo-Fernández reports financial support was provided by Principado de Asturias GRUPIN, co-financed by the Feder Programme of the European Union. Guillermo Redondo-Fernández reports financial support was provided by University of Oviedo.

Data availability

Data will be made available on request.

Acknowledgements

Guillermo Redondo-Fernández acknowledges his PhD grant (BP20-050) from the Asturias Regional Government (Spain). Alfredo de la Escosura-Muñiz acknowledges his "Ramón y Cajal" Research Fellow (RyC-2016-20299). This research was funded by Spanish Ministry of Science and Innovation (PID2020-117282RB-I00, MCI-20-PID2019-109698GB-I00 and MCI-21-PID2020-115204RB-I00), and by Principado de Asturias GRUPIN IDI/2021/000081 co-financed by the Feder Programme of the European Union. Authors would like to thank to Marcos García Ocaña from Biotechnology Preparative Unit for his advice, Marta Alonso Guervós for the help handling the confocal microscope and Angel Martinez Nistal for the development of the custom macro, both from Photonics Microscopy and Image Processing Unit of University of Oviedo.

Appendix A. Supplementary data

Supplementary data to this article can be found online at https://doi.org/10.1016/j.talanta.2024.126095.

References

[1] A.I. Barbosa, N.M. Reis, A critical insight into the development pipeline of microfluidic immunoassay devices for the sensitive quantitation of protein biomarkers at the point of care, Analyst 142 (2017) 858–882, https://doi.org/10.1039/C6AN02445A.
[2] A.L. Larraga-Urdaz, M.L. Fernandez Sanchez, J. Ruiz Encinar, J.M. Costa-Fernandez, Signal amplification strategies for clinical biomarker quantification using elemental mass spectrometry, Anal. Bioanal. Chem. 398 (2010) 1853–1859, https://doi.org/10.1007/s00216-021-03251-5.
[3] M. Polanski, N. Anderson, A list of candidate cancer biomarkers for targeted proteomics Biomark, Insights 1 (2006) 1–48, https://doi.org/10.1177/117727190600100001.
[4] L. Yang, J. Zheng, Z. Zou, H. Cai, P. Qi, Z. Qing, Q. Yan, L. Qiu, W. Tan, R. Yang, Human serum albumin as an intrinsic signal amplification amplifier for ultrasensitive assays of the prostate-specific antigen in human plasma, Chem. Commun. 56 (2020) 1843–1846, https://doi.org/10.1039/C9CC08501G.
[5] C.S. Thaxton, R. Elghanian, A.D. Thomas, S.I. Stoeva, J. Lee, N.D. Smith, A. J. Schaeffer, H. Klocker, W. Horninger, G. Bartsch, C.A. Mirkin, Nanoparticle-based bio-barcode assay redefines "undetectable" PSA and biochemical recurrence after radical prostatectomy, Proc. Natl. Acad. Sci. USA 106 (2009) 18437–18442, https://doi.org/10.1073/pnas.0904719106.
[6] F. Mannello, G. Gazzanelli, Prostate-specific antigen (PSA/hK3): a further player in the field of breast cancer diagnostics? Breast Cancer Res. 3 (2001) 238, https://doi.org/10.1186/bcr302.

[7] F.C. Mashkoor, J.N. Al-Asadi, L.M. Al-Naama, Serum level of prostate-specific antigen (PSA) in women with breast cancer, Cancer Epidemiol. 37 (5) (2013) 613–618, https://doi.org/10.1016/j.canep.2013.06.009.

[8] A.L. Larraga-Urdaz, M.L. Fernandez Sanchez, J. Ruiz Encinar, J.M. Costa-Fernandez, Signal amplification strategies for clinical biomarker quantification using elemental mass spectrometry, Anal. Bioanal. Chem. 414 (2022) 53–62, https://doi.org/10.1007/s00216-021-03251-5.

[9] L. Liu, D. Yang, G. Liu, Signal amplification strategies for paper-based analytical devices, Biosens. Bioelectron. 136 (2019) 60–75, https://doi.org/10.1016/j.bios.2019.04.043.

[10] Z. Rong, Q. Wang, N. Sun, X. Jia, K. Wang, R. Xiao, S. Wang, Smartphone-based fluorescent lateral flow immunoassay platform for highly sensitive point-of-care detection of Zika virus nonstructural protein 1, Anal. Chim. Acta 1055 (2019) 140–147, https://doi.org/10.1016/j.aca.2018.12.043.

[11] D. Li, D. Yao, C. Li, Y. Luo, A. Liang, G. Wen, Z. Jiang, Nanosol SERS quantitative analytical method: a review, TrAC, Trends Anal. Chem. 127 (2020) 115885, https://doi.org/10.1016/j.trac.2020.115885.

[12] R. Liu, X. Liu, Y. Tang, L. Wu, X. Hou, Y. Lv, Highly sensitive immunoassay based on Immunogold−Silver amplification and Inductively coupled plasma mass spectrometric detection, Anal. Chem. 83 (6) (2011) 2330–2336, https://doi.org/10.1021/ac103265z.

[13] P. Llano Suárez, M. García-Cortés, M.T. Fernández-Argüelles, J. Ruiz Encinar, M. Valledor, F.J. Ferrero, J.C. Campo, J.M. Costa-Fernández, Functionalized phosphorescent nanoparticles in (bio)chemical sensing and imaging – a review, Anal. Chim. Acta 1046 (2019) 16–31, https://doi.org/10.1016/j.aca.2018.08.018.

[14] M. García-Cortés, M.T. Fernández-Argüelles, J.M. Costa-Fernández, A. Sanz-Medel, Sensitive prostate specific antigen quantification using dihydrolipoic acid surface-functionalized phosphorescent quantum dots, Anal. Chim. Acta 987 (2017) 118–126, https://doi.org/10.1016/j.aca.2017.08.003.

[15] M. Garcia-Cortes, J. Ruiz Encinar, J.M. Costa-Fernandez, A. Sanz-Medel, Highly sensitive nanoparticle-based immunoassays with elemental detection: application to Prostate-Specific Antigen quantification, Biosens. Bioelectron. 85 (2016) 128–134, https://doi.org/10.1016/j.bios.2016.04.090.

[16] X. Li, B. Chen, M. He, G. Xiao, B. Hu, Gold nanoparticle labeling with tyramide signal amplification for highly sensitive detection of alpha fetoprotein in human serum by ICP-MS, Talanta 176 (2018) 40–46, https://doi.org/10.1016/j.talanta.2017.08.007.

[17] L. Cid-Barrio, J. Ruiz Encinar, J.M. Costa-Fernández, Catalytic gold deposition for ultrasensitive optical immunosensing of prostate specific antigen, Sensors 20 (2020) 5287, https://doi.org/10.3390/s20185287.

[18] S.C. Razo, N.A. Panferova, V.G. Panferov, I.V. Safenkova, N.V. Drenova, Y. A. Varitsev, A.V. Zherdev, E.N. Pakina, B.B. Dzantiev, Enlargement of gold nanoparticles for sensitive Immunochromatographic diagnostics of potato Brown rot, Sensors 19 (2019) 153, https://doi.org/10.3390/s19010153.

[19] G. Yang, Y. Lai, Z. Xiao, C. Tang, Y. Deng, Ultrasensitive electrochemical immunosensor of carcinoembryonic antigen based on gold-label silver-stain signal amplification, Chin. Chem. Lett. 29 (2018) 1857–1860, https://doi.org/10.1016/j.cclet.2018.11.030.

[20] A. de la Escosura-Muñiz, M. Maltez-da Costa, A. Merkoçi, Controlling the electrochemical deposition of silver onto gold nanoparticles: reducing interferences and increasing the sensitivity of magnetoimmuno assays, Biosens. Bioelectron. 24 (2009) 2475–2482, https://doi.org/10.1016/j.bios.2008.12.028.

[21] T. Ming-Hung Lee, H. Cai, I.H. Hsing, Effects of gold nanoparticle and electrode surface properties on electrocatalytic silver deposition for electrochemical DNA hybridization detection, Analyst 130 (2005) 364–369, https://doi.org/10.1039/B413143F.

[22] P. Zubiate, C.R. Zamarreño, P. Sánchez, I.R. Matias, F.J. Arregui, High sensitive and selective C-reactive protein detection by means of lossy mode resonance based optical fiber devices, Biosens. Bioelectron. 93 (2017) 176–181, https://doi.org/10.1016/j.bios.2016.09.020.

[23] L. Wang, W. Mao, D. Ni, J. Di, Y. Wu, Y. Tu, Direct electrodeposition of gold nanoparticles onto indium/tin oxide film coated glass and its application for electrochemical biosensor, Electrochem. Commun. 10 (2008) 673–676, https://doi.org/10.1016/j.elecom.2008.02.009.

[24] E.B. Aydın, M.K. Sezgintürk, Indium tin oxide (ITO): a promising material in biosensing technology, TrAC, Trends Anal. Chem. 97 (2017) 309–315, https://doi.org/10.1016/j.trac.2017.09.021.

[25] E.B. Aydın, M.K. Sezgintürk, A disposable and ultrasensitive ITO based biosensor modified by 6-phosphonohexanoic acid for electrochemical sensing of IL-1β in human serum and saliva, Anal. Chim. Acta 1039 (2018) 41–50, https://doi.org/10.1016/j.aca.2018.07.055.

[26] E.B. Aydın, M.K. Sezgintürk, An impedimetric immunosensor for highly sensitive detection of IL-8 in human serum and saliva samples: a new surface modification method by 6-phosphonohexanoic acid for biosensing applications, Anal. Biochem. 554 (2018) 44–52, https://doi.org/10.1016/j.ab.2018.05.030.

[27] D. Damborska, T. Bertok, E. Dosekova, A. Holazova, L. Lorencova, P. Kasak, J. Tkac, Nanomaterial-based biosensors for detection of prostate specific antigen, Microchim. Acta 184 (2017) 3049–3067, https://doi.org/10.1007/s00604-017-2410-1.

[28] S. Hu, H. Xu, B. Zhou, S. Xu, B. Shen, B. Dong, Z. Yin, S. Xu, L. Sun, J. Lv, J. Wang, W. Xu, X. Bai, L. Xu, S. Mintova, H. Song, Double stopband bilayer photonic crystal based upconversion fluorescence PSA sensor, Sensor. Actuator. B Chem. 326 (2021) 128816, https://doi.org/10.1016/j.snb.2020.128816.

[29] S.R. Nxele, R. Nkhahle, T. Nyokong, The synergistic effects of coupling Au nanoparticles with an alkynyl Co (II) phthalocyanine on the detection of prostate specific antigen, Talanta 237 (2022) 122948, https://doi.org/10.1016/j.talanta.2021.122948.

[30] E. Felici, M.D. Regiart, S.V. Pereira, F.G. Ortega, L. Angnes, G.A. Messina, M. A. Fernández-Baldo, Microfluidic platform integrated with carbon nanofibers-decorated gold nanoporous sensing device for serum PSA quantification, Biosensors 13 (2023) 390–403, https://doi.org/10.3390/bios13030390.

[31] X. Wang, X. He, Z. He, L. Hou, C. Ge, L. Wang, S. Li, Y. Xu, Detection of prostate specific antigen in whole blood by microfluidic chip integrated with dielectrophoretic separation and electrochemical sensing, Biosens. Bioelectron. 204 (2022) 114057, https://doi.org/10.1016/j.bios.2022.114057.

[32] Y. Dou, Z. Li, J. Su, S. Song, A portable biosensor based on Au nanoflower interface combined with electrochemical immunochromatography for POC detection of prostate-specific antigen, Biosensors 12 (2022) 259, https://doi.org/10.3390/bios12050259.

[33] F.G. Ortega, G.E. Gómez, C. González-Martinez, T. Valero, J. Expósito-Hernández, I. Puche, A. Rodriguez-Martinez, M.J. Serrano, J.A. Lorente, M.A. Fernández-Baldo, A novel, quick, and reliable smartphone-based method for serum PSA quantification: original design of a portable microfluidic immunosensor-based system, Cancers 14 (2022) 4483, https://doi.org/10.3390/cancers14184483.

[34] A.I. Barbosa, P. Gehlot, K. Sidapra, A.D. Edwards, N.M. Reis, Portable smartphone quantitation of prostate specific antigen (PSA) in a fluoropolymer microfluidic device, Biosens. Bioelectron. 70 (2015) 5–14, https://doi.org/10.1016/j.bios.2015.03.006.

[35] L. Trapiella-Alfonso, J.M. Costa-Fernandez, R. Pereiro, A. Sanz-Medel, Synthesis and characterization of hapten-quantum dots bioconjugates: application to development of a melamine fluorescentimmunoassay, Talanta 106 (2013) 243–248, https://doi.org/10.1016/j.talanta.2013.01.027.

[36] A. Ouhibi, A. Raouafi, N. Lorrain, M. Guendouz, N. Raouafi, A. Moadhen, Functionalized SERS substrate based on silicon nanowires for rapid detection of prostate specific antigen, Sensor. Actuator. B Chem. 330 (2021) 129352, https://doi.org/10.1016/j.snb.2020.129352.

[37] A. Bano, A. Dawood, Rida, F. Saira, A. Malik, M. Alkholief, H. Ahmad, M. Asad Khan, Z. Ahmad, O. Bazighifan, Enhancing catalytic activity of gold nanoparticles in a standard redox reaction by investigating the impact of AuNPs size, temperature and reductant concentrations, Sci. Rep. 13 (2023) 12359, https://doi.org/10.1038/s41598-023-38234-2.

[38] T.-M. Lee, H. Cai, I.-M. Hsing, Gold nanoparticle-catalyzed silver electrodeposition on an indium tin oxide electrode and its application in DNA hybridization transduction, Electroanalysis 16 (2004) 1628–1631, https://doi.org/10.1002/elan.200403039.

[39] Y. Xiao, S.N. Isaacs, Enzyme-linked immunosorbent assay (ELISA) and blocking with bovine serum albumin (BSA) - not all BSAs are alike, J. Immunol. Methods 384 (2012) 148–151, https://doi.org/10.1016/j.jim.2012.06.009.

[40] Z. Peterfi, B. Kocsis, Comparison of blocking agents for an ELISA for LPS, J. Immunoassay 21 (2000) 341–354, https://doi.org/10.1080/01971520009349541.

[41] G.L. Long, J.D. Winefordner, Limit of Detection. A closer look at the IUPAC definition, Anal. Chem. 55 (1983) 712A 724A, https://doi.org/10.1021/ac00258a724.

[42] J.N. Miller, J.C. Miller, Statistics and Chemometrics for Analytical Chemistry, sixth ed., Pearson Education Limited, England, 2010 (Chapter 5).

[43] L.I. Stowell, L.E. Sharman, K. Hamel, An enzyme-linked immunosorbent assay (ELISA) for prostate-specific antigen, Forensic Sci. Int. 50 (1991) 125–138, https://doi.org/10.1016/0379-0738(91)90141-5.

[44] A. Rahi, N. Sattarahmady, H. Heli, Label-free electrochemical aptasensing of the human prostate-specific antigen using gold nanospears, Talanta 156-157 (2016) 218–224, https://doi.org/10.1016/j.talanta.2016.05.029.

[45] S. Liu, Y. Huo, J. Bai, B. Ning, Y. Peng, S. Li, D. Han, W. Kang, Z. Gao, Rapid and sensitive detection of prostate-specific antigen via label-free frequency shift Raman of sensing graphene, Biosens. Bioelectron. 158 (2020) 112184, https://doi.org/10.1016/j.bios.2020.112184.

[46] W. Argoubi, A. Sánchez, C. Parrado, N. Raouafi, R. Villalonga, Label-free electrochemical aptasensing platform based on mesoporous silica thin film for the detection of prostate specific antigen, Sensor. Actuator. B Chem. 255 (2018) 309–315, https://doi.org/10.1016/j.snb.2017.08.045.

[47] A.V. Lakhin, V.Z. Tarantul, L.V. Gening, Aptamers: problems, solutions and prospects, Acta Naturae 5 (4) (2013) 34–43. PMID: 24455181; PMCID: PMC3890987.